

AD622573

AFCRL-65-457
JUNE 1965
SPECIAL REPORTS, NO. 27



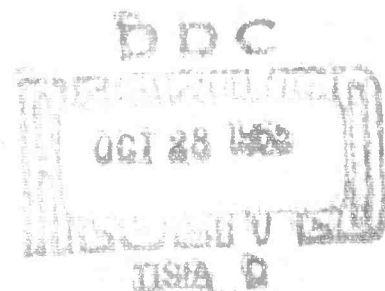
AIR FORCE CAMBRIDGE RESEARCH LABORATORIES

L. G. HANSCOM FIELD, BEDFORD, MASSACHUSETTS

Geophysical Implications of Shear Deformation in Rocks

ROBERT E. RIECKER

CLEARINGHOUSE FOR FEDERAL SCIENTIFIC AND TECHNICAL INFORMATION			
Hardcopy	Microfiche		
\$ 2.00	\$ 0.50	35 pp	12
ARCHIVE COPY			



OFFICE OF AEROSPACE RESEARCH
United States Air Force



**BEST
AVAILABLE COPY**

AFCRL-65-457
JUNE 1965
SPECIAL REPORTS, NO. 27

TERRESTRIAL SCIENCES LABORATORY PROJECT 7639

AIR FORCE CAMBRIDGE RESEARCH LABORATORIES

L. G. HANSCOM FIELD, BEDFORD, MASSACHUSETTS

Geophysical Implications of Shear Deformation in Rocks

ROBERT E. RIECKER

Sponsored by
Advanced Research Projects Agency
Project Vela-Uniform
ARPA Order No. 292

This research was supported by the Advanced Research Projects Agency,
Project Vela-Uniform Office and was monitored by AFCRL

OFFICE OF AEROSPACE RESEARCH
United States Air Force



BLANK PAGE

Abstract

A new shear press employing spherical opposed anvils is used to determine shear strength, coefficients of internal friction, and viscosity data for upper-mantle mineral analogues under geophysically realistic conditions of high temperature and pressure. The press uses high-frequency induction to externally heat samples to 1000°C at simultaneous pressures to 60 kb. Strain rates vary from 1 sec^{-1} to 10^{-3} sec^{-1} .

Torsion induced shear tests under normal pressures as high as 70 kb on forsterite, enstatite, labradorite, diopside, and pyrope garnet indicate that all these minerals possess very high strength at 27°C, but that their strength decreases markedly at higher temperatures. Sample behavior at strain rates of 10^{-3} sec^{-1} suggests further slight weakening.

Shear strengths for forsterite, enstatite, diopside, and labradorite equal 15.17, 14.92, 14.03, and 13.15 kb respectively at 50 kb normal pressure and 27°C, but decrease approximately 12 percent for each 250°C rise in temperature. Pyrope exhibits a strength of 19.47 kb at 69 kb normal pressure and 27°C. Variation in strain rate from 1 sec^{-1} to 10^{-3} sec^{-1} produces no detectable strength variation at 27°C, negligible effect in two tests at 300°C, and a 5 percent strength decrease in two tests at 700°C for natural forsterite from Addie, North Carolina.

Internal friction coefficients for forsterite, enstatite, diopside, labradorite, and pyrope are 0.11, 0.23, 0.17, 0.15, and 0.15 respectively at 27°C and decrease 0.01 each at 300°C. At 37 kb ± 1 kb normal pressure and 27°C temperature, rhombic enstatite inverts to the stable, high-temperature, monoclinic form of

clinoenstatite within minutes under the influence of shear stress. The monoclinic form persists at least to 800°C and 50 kb.

Less than 1 percent of weight by water released by serpentine dehydration associated with natural forsterite above 500°C produces a 20 percent decrease in strength in the olivine aggregate as temperature is raised from 300 to 520°C. Water weakening of olivine may be significant at earth depths ranging from 20 to 40 km.

Surfaces in contact under high pressures and low temperatures shear discontinuously by a process that creates and shears off microscopic junctions along the interface, and manifests in stick-slip behavior.

Under the experimental conditions, all five minerals deform cataclastically, with plastic behavior becoming important at high pressures and temperatures and at slow strain rates.

Foreword

This report is an abridgement of talks given by the author at the Earth Science Technologies Association Seminar, West Warwick, Rhode Island; the Air Force Institute of Technology, Wright-Patterson Air Force Base, Ohio; Boston College, Chestnut Hill, Mass.; the VESIAC Special Advisory Conference, LaJolla, California; and the Geology Department, University of Rochester, Rochester, New York. Minor changes have been made in the text in order to more clearly develop points that were made with visual aids during the talks.

BLANK PAGE

Contents

1. INTRODUCTION	1
2. CAUSES OF ROCK FAILURE	2
3. FACTORS INFLUENCING ROCK BEHAVIOR	2
4. ROCK DEFORMATION	4
5. ROCK-DEFORMATION TESTS	4
6. CURRENT ROCK-DEFORMATION RESEARCH AT AFCRL	6
7. EQUIPMENT USED FOR EXPERIMENTS	8
8. MINERALS USED IN EXPERIMENTS	10
9. RESULTS OF EXPERIMENTS	10
10. SUMMARY OF EXPERIMENTS	19
11. CONCLUSIONS	19
ACKNOWLEDGMENTS	21
REFERENCES	23

Illustrations

1. Stress-Strain Diagram Showing Difference in Behavior of Ductile and Brittle Substance	3
2. Stress-Strain Diagram Showing Effect of Compressive Stress on Behavior of Limestone	3
3. Stress-Strain Diagram Showing Effect of Temperature and Solutions on Strength of Limestone	5
4. Cross Section of Simple Opposed Anvil Apparatus	5
5. Schematic Diagram of a Piston and Cylinder Device	7
6. Schematic Drawing of Belt Type Pressure Apparatus	7
7. Photograph of Tetrahedral Press Located in Material Sciences Laboratory at AFCRL	7
8. Section of the Earth Showing Thin Outer Crust, Thick Intermediate Mantle, and Inner Core	9
9. Schematic Drawing of AFCRL Shear Press Capable of Simultaneous Pressures to 60 Kb and Temperatures to 1000°C	9
10. Photograph of AFCRL Shear Press with High-Frequency-Induction Heater to Left	11
11. Schematic Drawing of Anvil Assembly Showing Spherical Opposed Anvils	11
12. Photograph of Anvil Assembly Showing Infrared Pyrometer to Left	11
13. Composition Diagram Showing Rock Analog Analyzed	12
14. Shear Stress-Pressure Diagram Showing Initial Surficial Slip Followed by Region of Internal Flow	12
15. Shear Stress-Normal Pressure Curve for Olivine Minerals	12
16. Typical Extinction Band Group in Olivine	15
17. Thin Section of North Carolina Olivine Showing Serpentine Adjacent to and Along Cracks in the Olivine Grains	15
18. Shear Stress-Normal Pressure Curves for Enstatite Deformed to 700°C and 55 Kb Normal Pressure	16
19. Pressure-Temperature Diagram Showing Phases of Enstatite	16
20a. Typical Surface Relief on "Smooth" Surface	16
20b. Formation of Junction Upon Joining of Two "Smooth" Surfaces	16
21. Electron Micrograph of Deformed Olivine Pellet Showing Approximately Three Asperities per Square Micron	18
22. Diagram Showing Initial Elastic Deformation of the Asperity (A), Followed by Ductile Deformation (B) with Terminal Rupture Followed by General Strain Hardening (C)	18

Geophysical Implications of Shear Deformation in Rocks

1. INTRODUCTION

The purpose of this paper is to briefly describe the rock-deformation research being conducted by the U.S. Air Force. The research program was initiated under the Advanced Research Projects Agency's VELA-UNIFORM program, and its objective is to determine shear strength, viscosity, and internal friction data for deep crust and upper mantle rock and mineral analogues under geophysically realistic conditions of very high temperatures and pressures. The data obtained through this research will be, initially, used to interpret earthquake origin and seismic signal generation; ultimately, it will be used to determine criteria that can be utilized to distinguish between natural earth phenomena and underground explosions.

Even after 7 years of thought and experiment, it is still difficult to distinguish the natural from the man-made disturbances. For example, in 1962 (the last full year of major underground testing), 50 underground shots with a yield greater than 1 kt were detonated. In the same year over 12,500 earthquakes with magnitudes greater than 4 were recorded. If a geophysicist were to assume that every tremor observed by him was an earthquake, he would be right 99.6 percent of the time. He would be wrong only 0.4 percent of the time, but it's this minor inaccuracy that has such severe consequences in a test ban program.

(Received for publication 12 March 1965)

Although many problems remain, some encouraging progress has been made in the discrimination field. In 1958, when we first began seriously considering the possibility of a test ban, seismologists listed almost 500 events from the USSR which could have been classified as of unknown origin. In other words, one couldn't determine whether they were explosive tests or natural earthquakes. In 1964 the total of unknowns had dropped to around 40 — an impressive advance, although still a disturbing number of unknowns remains to be discriminated. This remainder will be tougher to crack.

2. CAUSES OF ROCK FAILURE

Part of our project in rock-deformation research involves obtaining a better understanding of rock failure and what actually causes earthquakes. Much has been learned at the Nevada test site and elsewhere relative to the phenomenology of underground explosions and the transfer of energy into elastic compressional and transverse waves, but very little is known about the origin of earthquakes or about rock behavior below the surface of the earth. The deepest oil well in west Texas penetrates only about 25,000 ft (about 5 miles) of the crust, the deepest mines in the world about 2 miles. This absolute dearth of information about the deeper crust and mantle is incredible when we recall the almost routine satellite flights to distant space hundreds of thousands or even millions of miles from us. The National Science Foundation's Project Mohole—for which a hole will be drilled to the boundary between the earth's crust and mantle—is a positive step toward alleviating the dearth of information.

Now let's review very briefly and generally what we do know about rock behavior in the deep earth. Rocks behave in diverse fashion as a function of manifold environmental factors. Figure 1 shows a stress-strain curve for a brittle material (curve B) in which an initial linear elastic portion is terminated abruptly by rupture.* However, under differing conditions the same rock material may behave in a ductile fashion (curve A) where the initial linear elastic portion passes through a yield point followed by a region of strain hardening with a final region of flow.

3. FACTORS INFLUENCING ROCK BEHAVIOR

Next we ask, what factors influence the behavior of rocks. Figure 2 is a stress-strain diagram for limestone in which the only variation in the series of tests

*Figures 1, 2, and 3 are from Billings, M. P. (1956) Structural Geology, Prentice-Hall, Englewood Cliffs, New Jersey, pp. 16, 19, and 22.

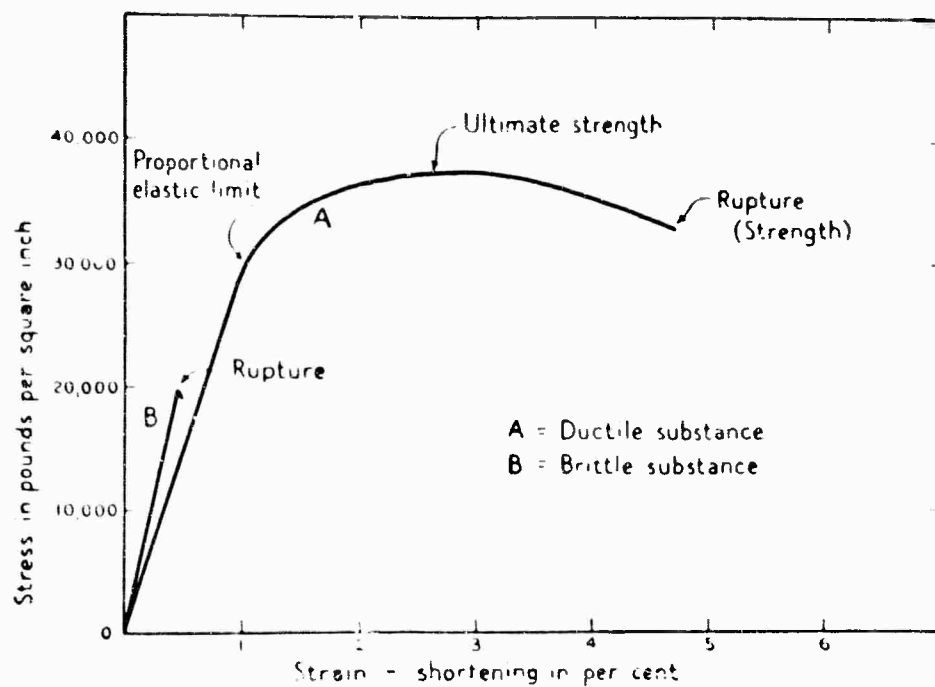


Figure 1. Stress-Strain Diagram Showing difference in Behavior of Ductile and Brittle Substance

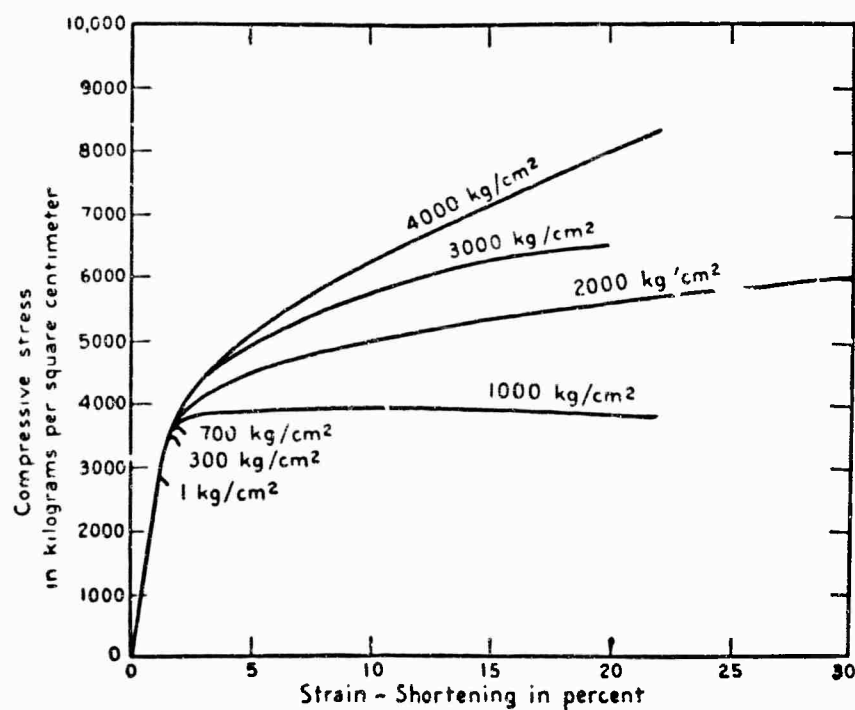


Figure 2. Stress-Strain Diagram Showing Effect of Compressive Stress on Behavior of Limestone

represented is pressure. Notice that in the initial test at 1 Kg/cm^2 the material is brittle. However, as the confining pressure increases, the curves reflect an increase in ductility, with the final test at 4000 Kg/cm^2 illustrating uniform flow.

Pressure is not the only factor that influences the strength of materials — temperature is also important. Figure 3 illustrates the effect of temperature on strength. Notice that for limestone again, temperatures from ambient to 150°C markedly decrease the strength of the limestone. Also in these tests, the presence of solutions caused further weakening of the rock.

Now to summarize some of the factors that effect the strength of materials. We have seen that pressure increases the strength of rocks and temperature decreases it. Time is also important. We know that if a rock is loaded quickly it will appear to be stronger than if it is loaded slowly, when creep or flow may occur. Rocks are strongest in compression, weakest in tension, and exhibit intermediate strengths in shear. Other factors that can further influence the behavior of rocks, but generally to a minor degree, are: nature of the stresses, presence of solutions, anisotropy and orientation, past strain history, crystal perfection, and aggregation.

4. ROCK DEFORMATION

Rocks deform in a number of ways. They deform macroscopically, exhibiting a phenomenon known as cataclasis that involves the smashing and rupture of the grains. They deform microscopically by gliding, which involves the movement of dislocations through the atomic structure of the material. The movement, generation, and blocking of dislocations that manifest in gliding constitute ductile flow. Rocks also deform through recrystallization. We'll discuss evidence for some of these flow mechanisms when we examine results from some of the specific shear tests, but now let's turn our attention to the manner in which rock-deformation tests are performed.

5. ROCK-DEFORMATION TESTS

There are four major types of apparatus used to apply pressures, temperatures, and variable strains to rock materials. The simplest type is the opposed anvil apparatus (Figure 4) in which a thin sample wafer is squeezed between two opposed pistons. This type of apparatus, first used by Bridgman, attains pressures of 400 kb and temperatures of 600 to 800°C . We'll see an offspring of this device a bit later, which we successfully use to 50 kb and 1000°C .

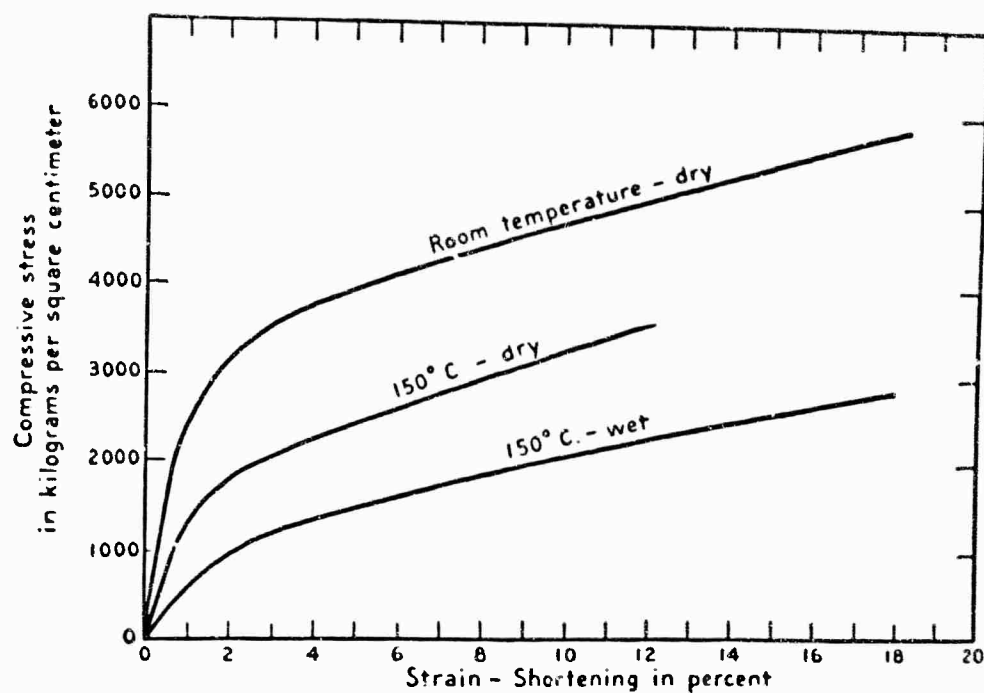


Figure 3. Stress-Strain Diagram Showing Effect of Temperature and Solutions on Strength of Limestone

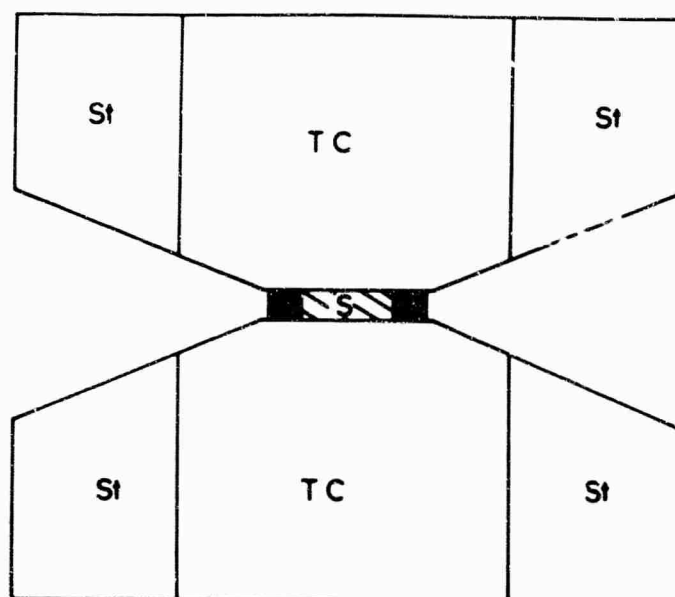


Figure 4. Cross Section of Simple Opposed Anvil Apparatus. TC = tungsten carbide, St = hardened steel binding rings, S = sample

Equally simple in design is the piston and cylinder device shown in Figure 5. The pressure exerted on the sample can be determined by the force per unit area of the piston. Maximum pressures of 400 kb at room temperature were obtained with this device by Drickamer at the University of Illinois. Heating to extreme temperatures is a problem in this device.

The belt apparatus (Figure 6), a more complex and elegant device, is said to be an ultimate design in using Bridgman's principle of massive support to prevent premature piston failure. This apparatus was designed by Tracy Hall at General Electric almost 10 years ago; today many similar apparatus are used to manufacture several million carats of diamonds every year. Its capacity exceeds 100 kb and 2000°C.

Another device designed by Hall at about the same time as the belt is the tetrahedral press. The one shown in Figure 7 is used routinely in the Materials Sciences Laboratory of AFCRL. Four rams arranged at the corners of a tetrahedron apply pressure to a sample placed in a tetrahedral shaped gasket of pyrophyllite. Very high pressure and temperatures, equivalent to those of the "belt", can be attained with this device.

Some experimenters added rams to the tetrahedral concept, and a new generation of cubic devices with six rams was developed. Press design reflects diverse engineering imagination required by the particular experiment. Shock techniques are also used to generate pressures in the megabar range—reaching earth-core pressures of 3.5 megabars for millionths of a second duration—but sustained pressures cannot be applied. Nevertheless, the correlation of static and dynamic test data has been very encouraging.

6. CURRENT ROCK-DEFORMATION RESEARCH AT AFCRL

For the remainder of our discussion, let's turn our attention to current rock-deformation research being conducted at AFCRL. As mentioned previously, we are concerned with the properties of the lower crust and upper mantle of the earth—in short, with the outer several hundred kilometers of the planet.

Figure 8 depicts a section of the earth exposing the thin crust that is separated from the bulky mantle which contains 7/8 of the earth's volume. The boundary called the Mohorovicic Discontinuity represents either a phase change from crust to denser polymorphs in the mantle, or a compositional change from lighter sialic rocks (with Si and Al predominating) to simatic rocks (with ferromagnesium minerals predominating) below. At 2900 km depth we find another geophysical and compositional boundary that marks the separation between the massive fluid core and the lighter rigid mantle. Why should the outer several hundred kilometers be so important?

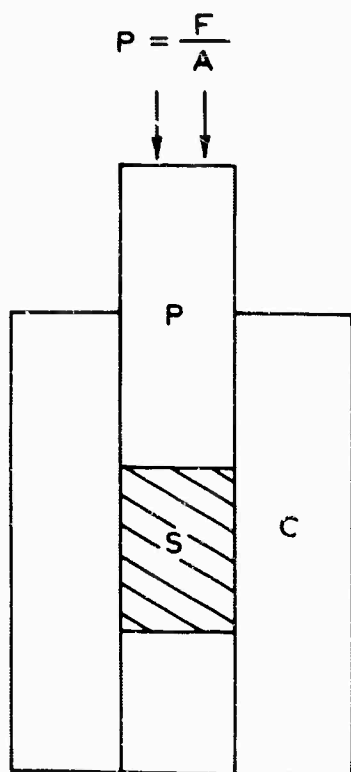


Figure 5. Schematic Drawing of a Piston and Cylinder Device. S = sample cavity

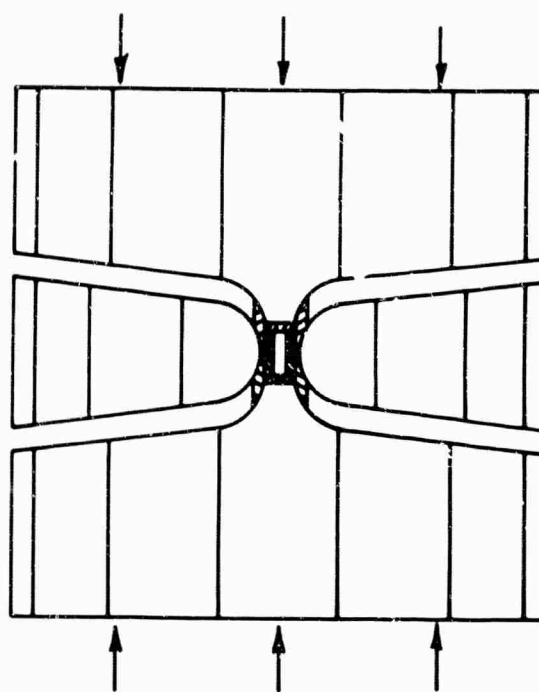


Figure 6. Schematic Drawing of Belt Type Pressure Apparatus

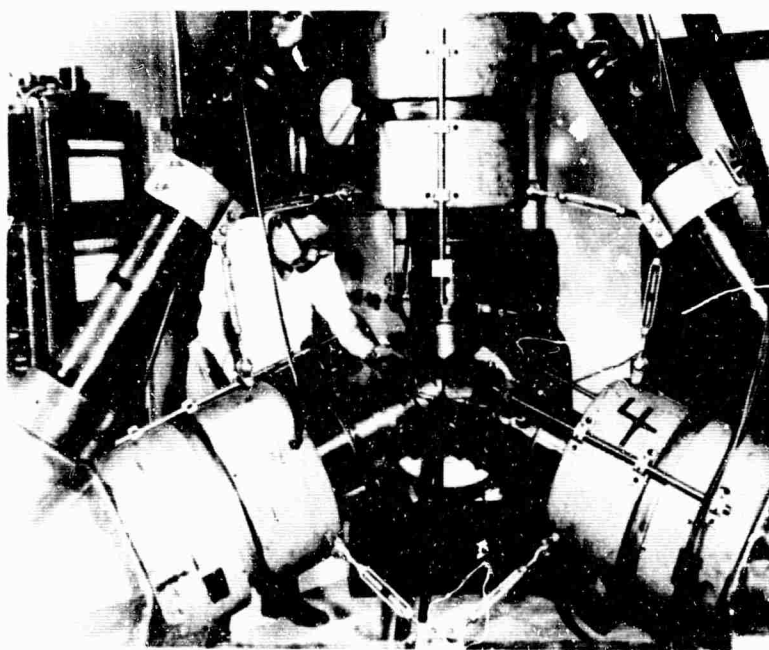


Figure 7. Photograph of Tetrahedral Press Located in Material Sciences Laboratory at AFCRL

Over 85 percent of earthquakes have focal depths at less than 200 km. The Gutenberg low-velocity channel lies at a depth between 150 and 400 km and represents a region within the mantle, possibly a phase change or liquifaction, in which the P and S waves decrease in velocity from an accelerating rate on entering the mantle. The Mohorovicic Discontinuity varies in depth from 80 km below young mountain chains to less than 10 km in the Pacific Ocean. Most magmas, or molten rocks and gases, that manifest in vulcanism and the emplacement of igneous rocks in the crust originate at depths less than 200 km. Frequently, the eruptions of Mauna Loa and Kilauea volcanoes in Hawaii are preceded by earthquakes, with focal depths at 60-70 km, several months or years prior to the eruptions. Finally, geodesists tell us from satellite data that the level of compensation also lies within this region, that is, all surface loads are fully balanced in the outer levels of the earth. Thus we see that the outer 200 km of the earth is an exceedingly interesting region. We could add other manifestations to our list, such as heat flow, which may be accounted for by radioactive decay in this outer region and none of which may represent conductive radiation from the molten core.

The outer earth holds as many profound secrets as does our neighbor the moon. Going into the outer earth by drilling is no more Jules Vernian than going to the moon by 1970, and it will be far less expensive, by at least 3 orders of magnitude. Although estimates vary depending upon the kinds of work included in the category "solid-earth research," by any estimate the total now being spent by federal agencies does not exceed a few tenths of 1 percent of the current yearly U.S. expenditure for research and development, now in the range of 15 billion dollars.* Now, right now, before we get completely carried away, let's turn our attention to the shear deformation program.

7. EQUIPMENT USED FOR EXPERIMENTS

The principal apparatus used in AFCRL shear experiments (Riecker, 1964a) is unique to rock-deformation research in three major respects: (1) its size and capacity, capable of simultaneous pressures and temperatures to 60 kb and 1000°C on 1-in. -diam samples approximately 0.020-in. -thick; (2) its use of high-frequency induction to quickly heat and quench samples; and (3) the radical design of its spherical anvils. (See Figure 9.)

The shear apparatus consists of a 1/2 hp motor and special three-pinion gear train, with change gears to provide sufficient torque to overcome shearing resistance in compressed mafic minerals at variable speeds from 10/sec to 10^{-3} /sec. (See Figure 10.) Normal pressure is generated by a 300-ton-capacity hydraulic jack that is used interchangeably with a 100-ton, controlled-clearance, frictionless jack.

*Solid Earth Geophysics, NAS-NRC Pub. No. 1231 (1964) p. 192.

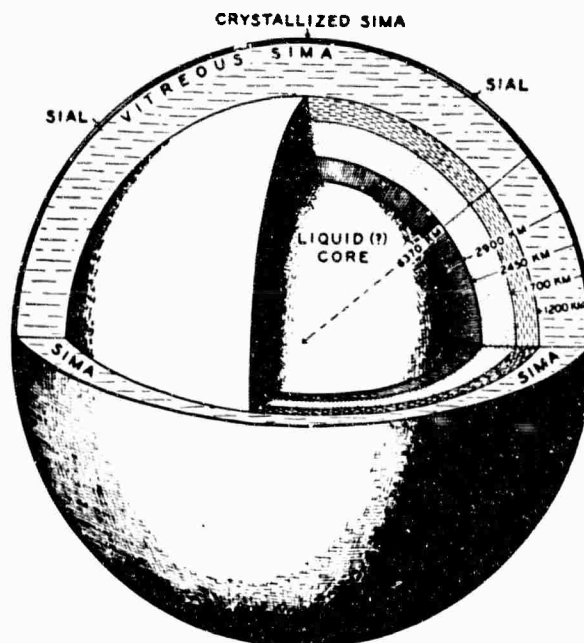


Figure 8. Section of the Earth Showing Thin Outer Crust, Thick Intermediate Mantle, and Inner Core. (The outer mantle is no longer considered to be vitreous as shown.)

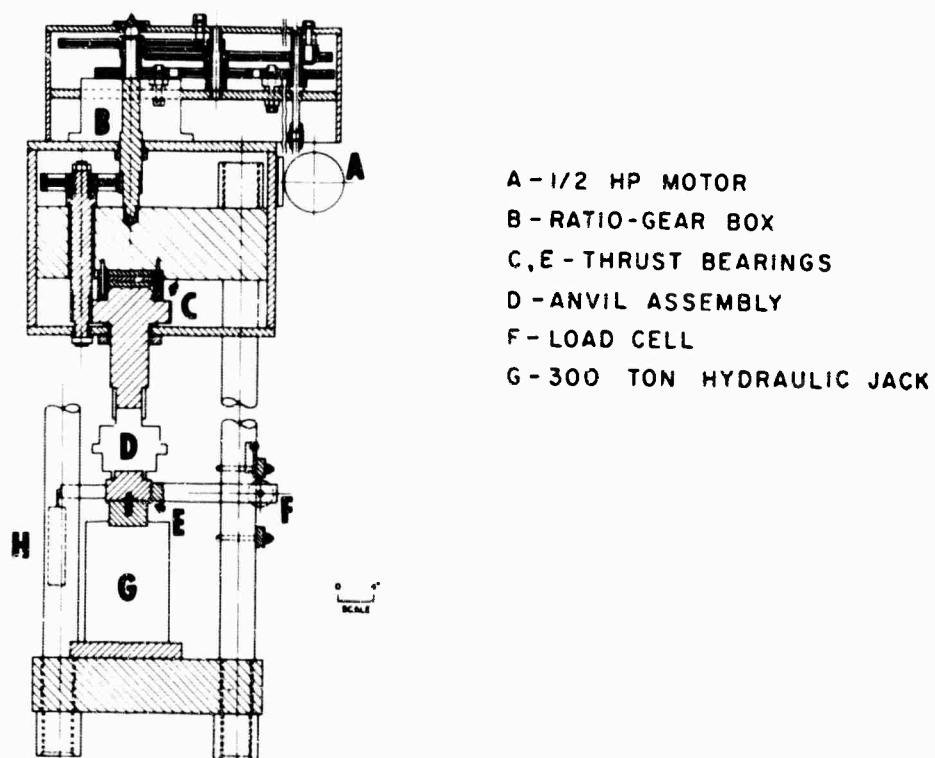


Figure 9. Schematic Drawing of AFCRL Shear Press Capable of Simultaneous Pressures to 60 kb and Temperatures to 1000° C

Load cells of various capacities at the end of a 15-in. -long torque arm monitor the force transmitted to the sheared sample. Shear strength is determined from the torque measurements. Heat is applied to the sample wafers through a 5-kw, high-frequency - induction heater. These experiments are modeled after those of Bridgman who, from 1920 to 1950, determined the shear strength of several hundred minerals, alloys, and compounds.

The spherical anvils used in shear experiments (Figure 11) are super-strength alloy and cermet balls that are forced into stainless steel and ceramic backup plates; they are cooled by water and liquid nitrogen. Massive support derives from the spherical geometry of the balls and the tight fit of the stainless steel surrounding their lower hemisphere. The balls are inexpensive, therefore economy is one of the major design attributes. The temperature of the sample under test conditions is monitored by an infrared pyrometer (Figure 12) that is calibrated against chromel-alumel thermocouples buried in exact duplicates of the anvils (Riecker, 1964b). Pressures and temperatures are accurate to within ± 1 percent at 50 kb and 1000°C. Also, maximum temperature of the sample can be reached within 50 sec from a cold start. Cooling to ambient temperatures requires somewhat less time.

8. MINERALS USED IN EXPERIMENTS

The minerals used in the shear tests are magnesium-olivine from Addie, North Carolina, and Hawaii; enstatite from Bamle, Norway; diopside; labradorite; and pyrope garnet. These minerals are the important constituents of peridotite or garnet pyrolyte, two rocks that have the appropriate seismic velocities and other physical and chemical properties for what is regarded as the dominant upper mantle rock phase (Figure 13). Synthetic boules of forsterite and diopside have been grown, using the Verneuil flame-fusion technique, and tested to determine the effect of variable composition within a single mineral and to minimize confusion resulting from spurious compositional variations.

Samples are prepared either by grinding the crystals into a powder and pressing the powder into pellets, or by thinly slicing the crystals. The method of sample preparation does not result in significant data variation. Each wafer is about 0.020-in. thick and may be 1/4 in., 1/2 in., or 1 in. diam.

9. RESULTS OF EXPERIMENTS

Bridgman (1937) showed, during a long series of shear experiments beginning about 1915, that a change in the shape of the shear-stress normal-pressure curve

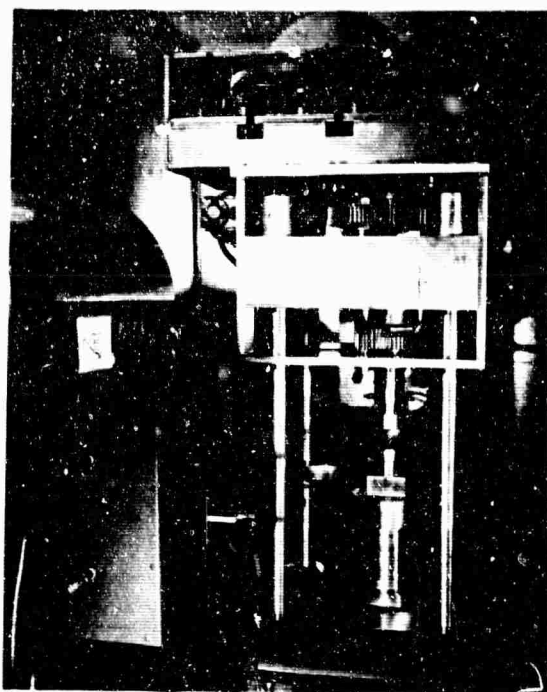


Figure 10. Photograph of AFCRL Shear Press With High-Frequency-Induction Heater to Left

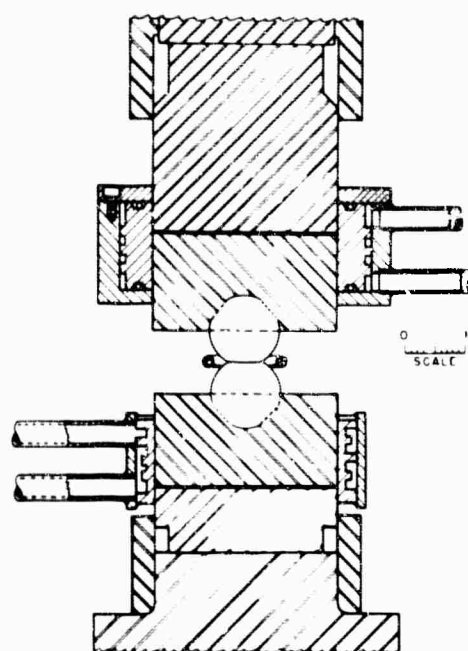


Figure 11. Schematic Drawing of Anvil Assembly Showing Spherical Opposed Anvils

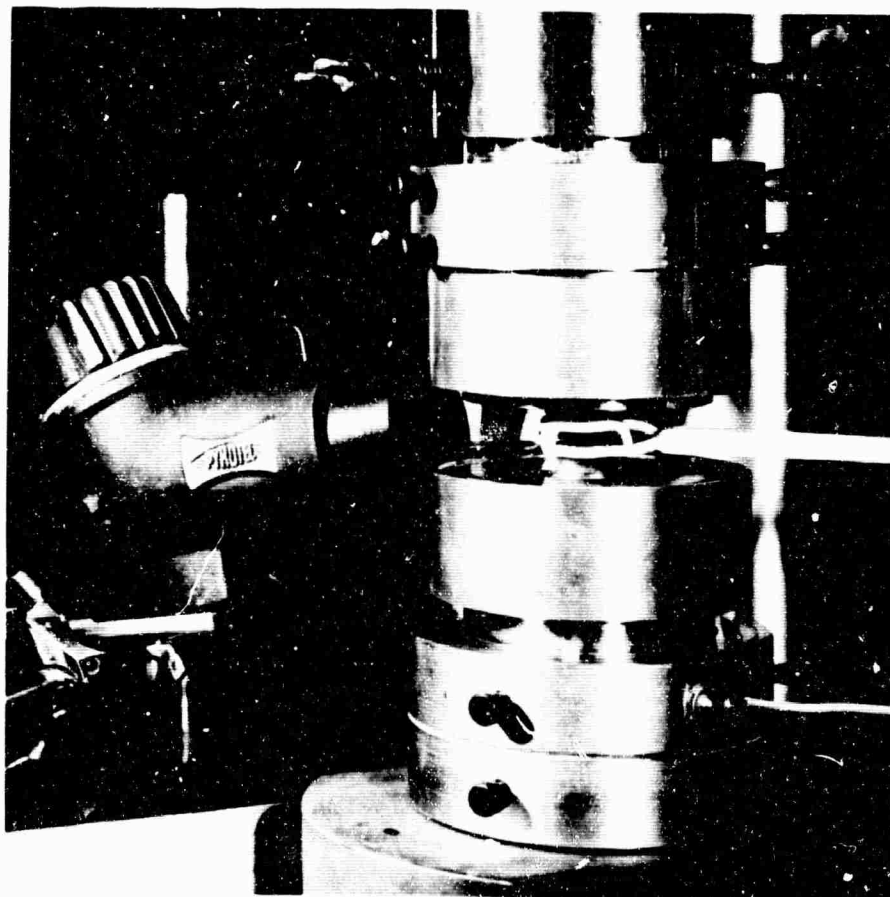


Figure 12. Photograph of Anvil Assembly Showing Infrared Pyrometer to Left

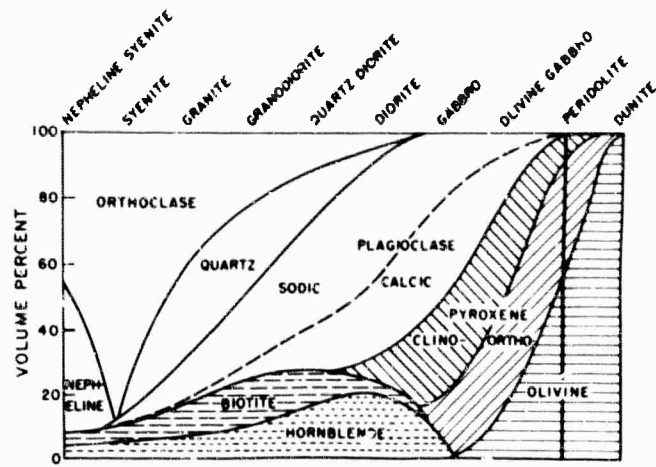


Figure 13. Composition Diagram Showing Rock Analog Analyzed (black vertical line)

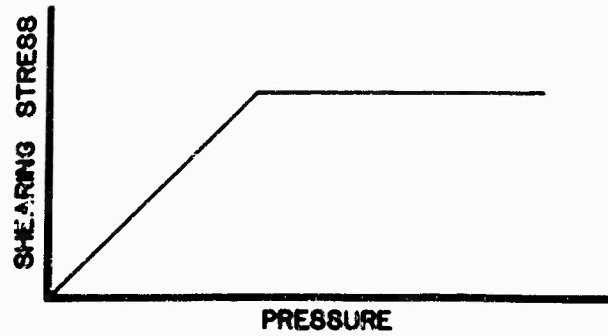


Figure 14. Shear Stress-Pressure Diagram Showing Initial Surficial Slip Followed by Region of Internal Flow

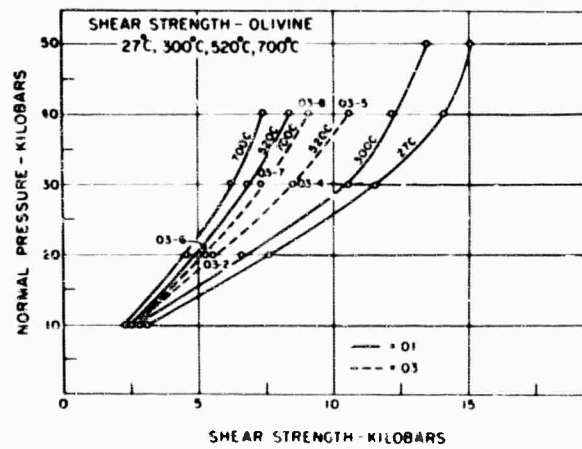


Figure 15. Shear Stress-Normal Pressure Curve for Olivine Minerals. 01=natural olivine from Addie, North Carolina, 03=synthetic forsterite

of a sheared sample marks the transition from surface slip of the anvils over the compressed wafer at low normal pressures to internal shear at high pressures (Figure 14). Theoretically, shear-stress normal-pressure curves should consist of two straight lines, one passing through the origin representing surficial slip, the other independent of normal pressure representing internal shear.

It's not surprising that the observed data produce curves that depart somewhat from this idealization. The dissimilarity may be considered a measure of the departure from the oversimplified model. The assumptions that ONLY surficial slip occurs below the knee and that ONLY true flow occurs above are obvious oversimplifications. The behavioral model is in fact complicated by the simultaneous occurrence of both these mechanisms, as well as by the predominant presence of cataclasis throughout the test conditions.

Figure 15 shows shear strength data plotted for forsterite at four temperatures from ambient to 700°C, up to 50 kb. Strain rate variation from 10/sec to 10^{-3} /sec produced negligible variation in the position of the data points. The dashed lines represent curves resulting from shear tests for synthetic Mg_2SiO_4 ; the solid lines record data for natural forsterite from North Carolina. True shear strength is represented by data from the upper portions of the curves, and may be approximated at lower pressures by extending the upper slope to intersect the abscissa.

Notice the decrease in relative strength between the 300°C curve and the 520°C curve for the natural forsterite. This decrease results from the decomposition or dehydration of from 4 to 5 percent of the associated serpentine, to talc plus water, which begins at about 500°C. The dehydration yields water vapor within the compressed pellet and manifests in significant pore pressure and strength reduction in the same manner as suggested by Hubbert and Rubey (1959). The effect is most prominent at high normal pressures where sample compression is greatest.

The synthetic forsterite shear results plot normally along curves, as would be expected for higher temperatures only. The difference between the strength of natural and synthetic forsterite at the same temperature amounts to almost 20 percent. This significant drop in strength represents one of the most important results of the research to date. It is similar in nature to observations by Griggs et al (1965) on synthetic quartz deformed at high temperatures.

Griggs found that the strength of synthetic quartz drops one-hundred-fold as the temperature is raised from 300°C to 600°C. He explains this anomalous weakness to be due to diffused water throughout the crystal which hydrolyzes the silicon-oxygen bonds. The silanol groups so formed become mobile at the higher temperatures and align themselves in dislocation lines. These move through the crystal with the dislocations under small applied shear stresses. Griggs has also observed similar water-weakening in quartz crystals surrounded by hydrous pressure media.

Similar examples of serpentine water-weakening were reported by Robertson (1964) and Handin (1964) for samples from the AMSOC experimental test hole in

Puerto Rico. Handin's samples under confining pressures to 2 kb showed a 60 per cent reduction in strength at temperatures from 20°C to 200°C. Heard (1963) observed a 10-fold strength reduction in gypsum as it passed through the transition to anhydrite plus water.

All of these observations of course raise the possibility of great weakness in the earth's deeper crust and upper mantle at temperatures very much less than the melting point of the rocks present there.

Internal deformation of sheared minerals at high pressures is indicated by the development of deformation lamellae, increased undulose extinction, and related X-ray, petrographic, and electron microscope features. Figure 16 shows a typical extinction band group developed in the Hawaiian olivine subparallel to (100). No evidence for recrystallization has been found. The failure mechanism is almost entirely cataclastic over the entire range of conditions. Data for high temperatures and pressures and for the slowest strain rates suggest a tendency for olivine to become ductile.

Figure 17, a thin section of natural North Carolina olivine, shows the minor associated antigorite and crysotile serpentine surrounding and along cracks in the forsterite grains. The hydrous minerals dehydrate over the temperature range from 500°C to 800°C. Less than 1 percent by weight of water is released, but even that small amount is sufficient to markedly affect the strength of the olivine.

Figure 18 illustrates a second important phenomenon that sometimes develops in shear experiments. It shows the results for enstatite that was deformed at temperatures, pressures, and strain rates similar to those applied to the olivine sample. On the ambient temperature curve, notice the effect on shear strength of a phase change as enstatite inverts at about 37 kb to the monoclinic polymorph clinoenstatite, which is stronger than the rhombic form under similar test conditions. Enstatite held at 80 kb for 1 hour without shear, however, does not invert, thus indicating that the inversion is shear sensitive. Shear causes the reaction to go almost to completion in 1 to 2 seconds at 39 kb.

These results differ from those obtained by Sclar (1964) for pure enstatite compressed hydrostatically in a modified belt apparatus at pressures and temperatures to 130 kb and 1300°C. Sclar's equilibrium boundary is shown and should be inferred to be below 15 kb. Notice that our samples, sheared considerably above the hydrostatic equilibrium boundary, still exhibit the clinoenstatite structure (Figure 19). This result indicates that shear stress may have a very significant effect on the phase transformations anticipated in the upper mantle. In this case the effect of shear is equivalent to several hundred degrees centigrade in facilitating the inversion of rhombic enstatite to the monoclinic high-temperature form. Also, in the future, considerably more care will have to be given to considerations of the nature and magnitude of stresses developed in experimental phase work.



Figure 16. Typical Extinction Band Group in Olivine. Extinction bands subparallel to (100). Diameter of grain is 2 mm



Figure 17. Thin Section of North Carolina Olivine Showing Serpentine Adjacent to and Along Cracks in the Olivine Grains. Largest grains are 2 mm across

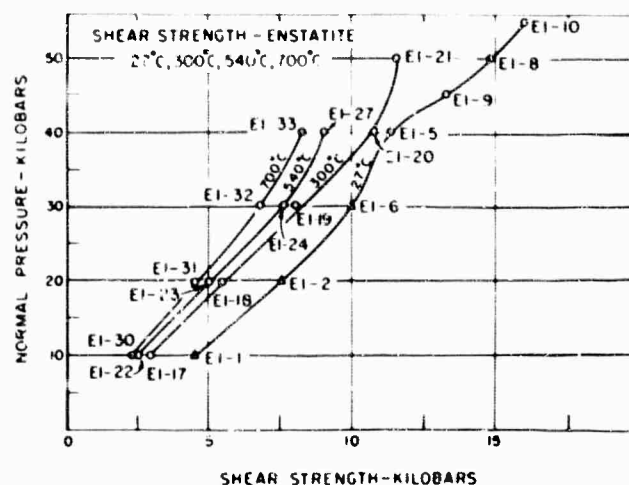


Figure 18. Shear Stress-Normal Pressure Curves for Enstatite Deformed to 700°C and 55 kb Normal Pressure

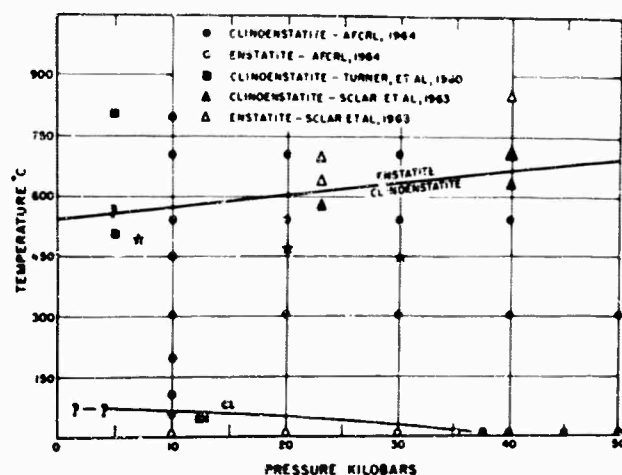


Figure 19. Pressure-Temperature Diagram Showing Phases of Enstatite. Upper boundary after Sclar (1963). Stars indicate pressure tests only, without shear. Solid symbols represent clinoenstatite, open symbols represent enstatite (rhombic polymorph)

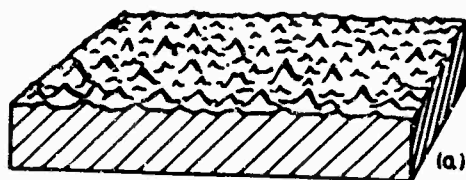


Figure 20a. Typical Surface Relief on "Smooth" Surface

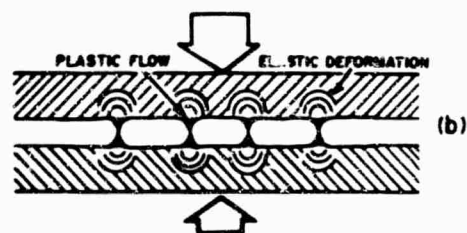


Figure 20b. Formation of Junctions Upon Joining of Two "Smooth" Surfaces

Our results show that enstatite inverts to clinoenstatite at very slight temperatures under the influence of shear stress, and that this monoclinic form persists to the limit of current experiments at 800°C and 50 kb.

One additional experiment manifestation might be of interest. Bridgman commented on a phenomenon common to his shear experiments, which he suggested might be of possible geophysical interest. He noted that in about 40 percent of the materials deformed, shear took place discontinuously with the evolution of loud snapping or chattering noises. Bridgman (1937) said: "Instead of rotating smoothly, many substances rotate with protest. Some substances chatter, others squeak, others make a grinding noise, and one has been found to hiss." He suggested that the snapping was a manifestation of internal rupture.

Snapping accompanies all our shear experiments at low temperatures, but diminishes and disappears entirely at temperatures above 400°C or at slower strain rates. We know now, much through the work of Bowden and Tabor (1960), that when two surfaces meet they join at only a few points of contact or asperities on each surface, and that these asperities deform when carrying the load (Figure 20). Joining two surfaces has been compared to placing Switzerland upside down over Austria. If the surfaces are sheared, then the asperities shear off while new points of contact weld. The snapping, therefore, represents the shearing of asperities and rewelding during shear.

Figure 21 is an electron micrograph of the surfaces of sheared olivine showing about three asperities per square micron. The continual shearing of the junctions and formation of new points of contact result in the observed stick-slip behavior noted in the torque record. Thus when load is applied to a sample pellet, junctions form at the asperities. The junctions flow sufficiently to carry the load while the substrate is loaded elastically. When shear begins the junctions are already ductile; therefore, the smallest tangential force produces minute tangential displacement or microslip in the junctions, and the joints grow and deform further. If the shear stress exceeds the shear strength of the material, the junctions fail and the surfaces slip over each other a minute distance until the process of penetration and cold welding recurs.

The sequence is shown diagrammatically in Figure 22, where A represents the initial elastic deformation of the asperity, B represents the ductile deformation of the junction, and C represents slip following rupture of the junctions, followed by general strain hardening at the interface.

As long as the contacting surfaces remain free of oxides or other contaminants, the stick-slip, jerky phenomenon characterizes the shear behavior along the interface. However, if contaminants are present, such as in the high-temperature shear experiments where anvil components readily oxidize, then the stick-slip snapping ceases and shear occurs only in the film separating the adjacent surfaces.



Figure 21. Electron Micrograph of Deformed Olivine Pellet Showing Approximately Three Asperities per Square Micron. Deep grooves result from shearing motion

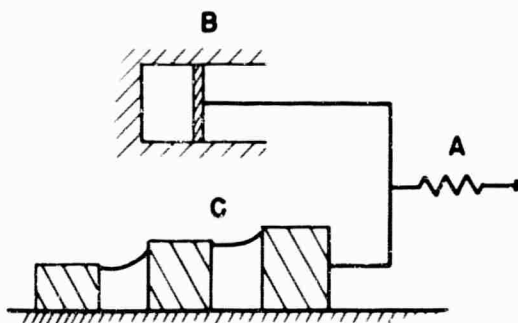


Figure 22. Diagram Showing Initial Elastic Deformation of the Asperity (A), Followed by Ductile Deformation (B) With Terminal Rupture Followed by General Strain Hardening (C)

At deep levels within the earth, stick-slip surely must accompany the shear of adjacent blocks joined along a planar interface, if indeed such a mechanism operates to generate elastic waves.

10. SUMMARY OF EXPERIMENTS

To summarize the major results of shear experiments to date, we have seen that pressures of from 10 to 50 kb increase the shear strength of mafic minerals by as much as 50 percent. Temperature decreases strength, generally by 12 percent at maximum pressures for each increase of 250°C. The rate of strain does not appear to affect shear strength significantly over the range from 10/sec to 10^{-3} /sec, but it should be noted that these strain rates are rapid and, as Heard (1963) has shown for Yule marble, strain rate effects become significant at rates less than 10^{-5} /sec above 400°C. It is almost certain that our strain rates favor cataclasis. Geologic strain rates are considered to be on the order of 10^{-14} /sec.

Shear stress facilitates phase transformations, as witnessed by the inversion of enstatite to clinoenstatite within seconds at 37 kb normal pressure and 27°C, whereas simple compression to 80 kb for extended periods does not effect the transformation. Compression tests held for 1 hour at 450°C also do not show inversion.

Less than 1 percent by weight of water released by dehydration of serpentine above 500°C produces a 30 percent decrease in strength in the olivine aggregate as the temperature is raised from 300°C to 520°C. This effect might be expected to be important at depths in the earth ranging from 20 to 40 km.

Surfaces in contact under high pressures shear discontinuously by a process that creates and shears off minute junctions along the contact interface and manifests in stick-slip behavior or "stiction". Finally, under the experimental conditions, olivine and enstatite—as well as the other minerals we did not discuss, deformed cataclastically, with the ductile behavior becoming important only at high pressures and temperatures and at slow strain rates.

11. CONCLUSIONS

The results of the experiments lead us to join other experimenters (Ode, 1960; Orowan, 1960, 1964; Griggs and Handin, 1960; Evison, 1963; Benioff, 1964) who suggest that deep earthquakes do not occur by the same process that we assume to exist at shallow earth depths. For as many have shown, the increase in strength as a function of pressure alone is sufficient to negate the existence of any reasonable stress couple that could cause strictly brittle fractures at deep levels. Further,

rocks change in behavior so completely with temperature, state of stress, solutions, and additional factors, and become so ductile at depth, that no sizeable stress couple could develop before ductile flow would dissipate the stress. In short, geologic faults probably do not exist at deep earth levels, and earthquakes, therefore, originate from other causes below shallow depths.

These observations — when coupled with the lack of any certain theory of rock strength, the observations of deep earthquakes to 700 km, and the interpretations therefrom — indicate that a significant problem still exists in earth physics. It is hoped that scientists and engineers will aggressively come to the aid of the experimenters by suggesting sounder and more realistic experiments for future geophysically oriented rock-deformation studies. A unified approach must be developed before the phenomenology of deep earthquakes is mastered.

Acknowledgments

The Advanced Research Projects Agency of the Department of Defense provided funds for the fabrication of the shear press as part of VELA-UNIFORM under contract No. AF19(628)-1646. The author is grateful to Dr. N. A. Haskell of AFCRL for his assistance and to Helen Cook, David Pendleton, and Roger Landers for their technical assistance.

Thanks are due to Thomas McKeon of the Army Map Service; James Vary of Boston College; Dr. J. DeNoyer and T. W. Caless of VESIAC and the University of Michigan; Captains Stewart Johnson and Shelton Alexander of The Air Force Institute of Technology; and Dr. Taro Takahashi of the University of Rochester for invitations to speak before their respective groups and for their excellent cooperation.

BLANK PAGE

References

- Benioff, H. (1964) Earthquake source mechanisms, Science 143:1399-1406.
- Bowden, F.P., Tabor, D. (1960) Friction and Lubrication, Methuen & Co., London, p. 1-150.
- Bridgman, P.W. (1937) Shearing phenomena at high pressures, particularly in inorganic compounds, Proc. Am. Acad. Arts Sci. 71 (No. 9):387-460.
- Bridgman, P.W. (1937) Flow phenomena in heavily stressed metals, Jour. App. Phys. 8:328-336.
- Evison, F.F. (1963) Earthquakes and faults, Bull. Seismol. Soc. Am. 53:873-891.
- Griggs, D.T., Handin, J. (1960) Observations on fracture and a hypothesis of earthquakes, Geol. Soc. Am. Memoir 79, p. 347-364.
- Griggs, D.T., Blacic, J.D. (1965) Quartz: Anomalous weakness of synthetic crystals, Science 147:292-295.
- Handin, J. (1964) Strength at high confining pressure and temperature of serpentine from Malaguez, Puerto Rico, in A Study of Serpentinite NAS-NRC Pub. 1188, p. 126-131.
- Heard, H.C. (1963) Effect of large changes in strain rate in the experimental deformation of Yule Marble, Jour. Geol. 71:162-195.
- Hubbert, M.K., Rubey, W.W. (1959) Role of fluid pressures in mechanics of overthrust faulting, Bull. Geol. Soc. Am. 70 (No. 2):115-206.
- Ode, H. (1960) Faulting as a velocity discontinuity of plastic deformation, Geol. Soc. Am. Memoir 79, p. 292-322.
- Orowan, E. (1960) Mechanism of seismic faulting, Geol. Soc. Am. Memoir 79, p. 323-346.
- Orowan, E. (1964) The mechanical properties of the earth, continental drift, and the origin of mountains, Science 146:1003-1010.
- Riecker, R.E. (1964a) New shear apparatus for temperatures of 1000°C and pressures of 50Kb, Rev. Sci. Instr. 35 (No. 5):596-598.

- Riecker, R.E. (1964b) Use of induction heating in rock deformation apparatus, Rev. Sci. Instr. 35 (No. 7):1232-1236.
- Robertson, E.C. (1964) Strengths and elastic moduli of serpentinite from Mayaguez, Puerto Rico, in A study of Serpentinite, NAS-NRC Pub. 1188, p. 118-125.
- Sclar, C.B. (1964) High pressure studies in the system MgO-SiO₂ and the constitution of the upper mantle, Bull. Am. Assoc. Petrol. Geol. 48 (No. 4):546.

SPECIAL REPORTS

- No. 1. Today's Meteorological Rocket Network and Atmospheric Problems of Aerospace Vehicles, *Norman Sissenuwine, May 1964 (REPRINT)*.
- No. 2. Ferrimagnetic Resonance Relations for Magnetocrystalline Anisotropy in Cubic Crystals, *Hans Roland Zapp, April 1964*.
- No. 3. Worldwide Collection and Evaluation of Earthquake Data, Final Report on Evaluation of 1960 Seismicity, *R.L. Fisher, R.G. Baker, and R.R. Guidroz, June 1964*.
- No. 4. Visual Observations Beneath a Developing Tornado, *Ralph J. Donaldson, Jr., and William E. Lamkin, August 1964 (REPRINT)*.
- No. 5. Bibliography of Rock Deformation, *R.E. Riecker, 1/Lt, USAF, September 1964*.
- No. 6. The Modification of Electromagnetic Scattering Cross Sections in the Resonant Region, A Symposium Record, Volume I, *J.K. Schindler, 1/Lt, USAF, R.B. Mack, Editors, September 1964*.
- No. 6. The Modification of Electromagnetic Scattering Cross Sections in the Resonant Region (U), A Symposium Record, Volume II, *J.K. Schindler, 1/Lt, USAF, R.B. Mack, Editors, September 1964 (SECRET)*.
- No. 7. The Natural Environment for the Manned Orbiting Laboratory System Program (MOL), *25 October 1964*.
- No. 8. The Vertical Transfer of Momentum and Heat At and Near the Earth's Surface, *Morton L. Barad, October 1964 (REPRINT)*.
- No. 9. Bibliography of Lunar and Planetary Research—1963, *J.W. Salisbury, R.A. VanTassei, J.E.M. Adler, R.T. Dodd, Jr., and V.G. Smalley, November 1964*.
- No. 10. Hourly Rawinsondes for a Week (Part II), *Arnold A. Barnes, Jr., and Henry A. Salmela, November 1964*.
- No. 11. An Appraisal of Rayleigh, *John Howard, Editor, November 1964 (REPRINT)*.
- No. 12. Communication by Electroencephalography, *E.M. Dewan, November 1964*.
- No. 13. Proceedings of AFCRL Workshop on 20 July 1963 Solar Eclipse, *J.A. Klobuchar and R.S. Allen, Editors, December 1964*.
- No. 14. Continuous Zone Refining, *John K. Kennedy and N. Grier Parke, III, December 1964*.
- No. 15. Applications of Lasers, *C. Martin Stickley, November 1964*.
- No. 16. On the Physical Necessity for General Covariance in Electromagnetic Theory, *E.J. Post, December 1964*.
- No. 17. A Compendium of Papers in the Fields of Wave Propagation and Geotechnics Prepared at AFCRL During 1963, *Owen W. Williams, December 1964*.
- No. 18. A Compendium of Papers in the Fields of Geodesy and Planetary Geometry Prepared at AFCRL During 1963, *Owen W. Williams, Editor, January 1965*.
- No. 19. Study of Ferrimagnetic Crystals by Parallel Pumping, *James C. Sethares and Frank A. Olson, January 1965*.
- No. 20. Studies of the Characteristics of Probable Lunar Surface Materials, *John W. Salisbury and Peter E. Glaser, Editors, January 1964*.
- No. 21. Research in Computer Sciences, *Hans H. Zschirnt, February 1965 (REPRINT)*.
- No. 22. Airglow Calibrations Symposium, *C.J. Hernandez and A.L. Carrigan, December 1964*.
- No. 23. An Introduction to the Geology of the Moon, *Luciano B. Ronca, May 1965*.
- No. 24. Ultrapurification, Its Attainment and Analysis, *A.F. Armington, B. Rubin, and J. Paul Cali, June 1965 (REPRINT)*.
- No. 25. A Bibliography of the Electrically Exploded Conductor Phenomenon, Supplement No. 1, *William G. Chace and Eleanor M. Watson, June 1965*.
- No. 26. Observations on Solar Flares, *John T. Jefferies, Frank Q. Orrall, Josip Kleczek, Hermann U. Schmidt, and Anton Bruzek, June 1965 (REPRINT)*.
- No. 27. Geophysical Implications of Shear Deformation in Rocks, *Robert E. Riecker, June 1965*.

BLANK PAGE

DOCUMENT CONTROL DATA - RAD

(Security classification of title, body of abstract and indexing annotation must be entered when the overall report is classified)

1. ORIGINATING ACTIVITY (Corporate author) Hq AFCRL, OAR (CRJ) United States Air Force Bedford, Massachusetts		2a. REPORT SECURITY CLASSIFICATION Unclassified	
		2b. GROUP -	
3. REPORT TITLE Geophysical Implications of Shear Deformation in Rocks			
4. DESCRIPTIVE NOTES (Type of report and inclusive dates) Scientific Report. State of the art.			
5. AUTHOR(S) (Last name, first name, initial) RIECKER, Robert E.			
6. REPORT DATE June 1965		7a. TOTAL NO. OF PAGES 36	7b. NO. OF REFS 17
8a. CONTRACT OR GRANT NO. -		9a. ORIGINATOR'S REPORT NUMBER(S) AFCRL-65-457	
b. PROJECT AND TASK NO. 7639-05			
c. OOD ELEMENT 62405394		9b. OTHER REPORT NO(S) (Any other numbers that may be assigned this report) AFCRL-65-457	
d. OOD SUBELEMENT 681000			
10. AVAILABILITY/LIMITATION NOTICES Qualified requestors may obtain copies of this report from DDC. Other persons or organizations should apply to the Clearinghouse for Federal Scientific and Technical Information (CFSTI), Sills Building, 5285 Port Royal Road, Springfield, Virginia 22151.			
11. SUPPLEMENTARY NOTES ARPA No. 292		12. SPONSORING MILITARY ACTIVITY Hq AFCRL, OAR (CRJ) United States Air Force Bedford, Massachusetts	
13. ABSTRACT A new shear press employing spherical anvils has been used to determine shear strength, internal friction, and viscosity data for upper-mantle mineral analogues under geophysically realistic conditions of high temperature and pressure. The press uses high-frequency induction to externally heat samples to 1000°C at 50 kb pressure. Strain rates vary from 1/sec to 10 ⁻³ /sec. Shear under normal pressures to 70 kb indicates that forsterite, enstatite, labradorite, diopside, and pyrope all yield high strengths at 27°C, but that strength decreases at higher temperatures. Shear strengths for forsterite, enstatite, diopside, and labradorite equal 15.17, 14.92, 14.03, and 13.15 respectively at 50 kb pressure and 27°C, but decrease 12 percent for each 250°C temperature rise. Pyrope exhibits a strength of 19.47 kb at 69 kb pressure and 27°C. At 37 kb pressure and 27°C, enstatite inverts to the stable high-temperature monoclinic form clinoenstatite, within minutes under the influence of shear stress. Less than 1 percent by weight of water released by serpentine dehydration associated with natural forsterite above 500°C produces a 20 percent strength decrease. Under the experimental conditions, all five minerals deform cataclastically, with plastic behavior becoming important at high pressures and temperatures and at slow strain rates.			

14.	KEY WORDS	LINK A		LINK E		LINK C	
		ROLE	WT	ROLE	WT	ROLE	WT
	Geophysics Shear strenght Rocks Seismology						

INSTRUCTIONS

1. ORIGINATING ACTIVITY: Enter the name and address of the contractor, subcontractor, grantee, Department of Defense activity or other organization (corporate author) issuing the report.

2a. REPORT SECURITY CLASSIFICATION: Enter the overall security classification of the report. Indicate whether "Restricted Data" is included. Marking is to be in accordance with appropriate security regulations.

2b. GROUP: Automatic downgrading is specified in DoD Directive 5200.10 and Armed Forces Industrial Manual. Enter the group number. Also, when applicable, show that optional markings have been used for Group 3 and Group 4 as authorized.

3. **REPORT TITLE:** Enter the complete report title in all capital letters. Titles in all cases should be unclassified. If a meaningful title cannot be selected without classification, show title classification in all capitals in parenthesis immediately following the title.

4. **SCRIPTIVE NOTES:** If appropriate, enter the type of report, e.g., interim, progress, summary, annual, or final. Give the inclusive dates when a specific reporting period is covered.

5. **AUTHOR(S):** Enter the name(s) of author(s) as shown on or in the report. Enter last name, first name, middle initial. If military, show rank and branch of service. The name of the principal author is an absolute minimum requirement.

6. **REPORT DATE:** Enter the date of the report as day, month, year, or month, year. If more than one date appears on the report, use date of publication.

7a. TOTAL NUMBER OF PAGES: The total page count should follow normal pagination procedures, i.e., enter the number of pages containing information.

7b. NUMBER OF REFERENCES: Enter the total number of references cited in the report.

8a. **CONTRACT OR GRANT NUMBER:** If appropriate, enter the applicable number of the contract or grant under which the report was written.

8b, 8c, & 8d. PROJECT NUMBER: Enter the appropriate military department identification, such as project number, subproject number, system numbers, task number, etc.

9a. ORIGINATOR'S REPORT NUMBER(S): Enter the official report number by which the document will be identified and controlled by the originating activity. This number must be unique to this report.

96. OTHER REPORT NUMBER(S): If the report has been assigned any other report numbers (either by the originator or by the sponsor), also enter this number(s).

10. AVAILABILITY/LIMITATION NOTICES: Enter any limitations on further dissemination of the report, other than those imposed by security classification, using standard statements such as:

- (1) "Qualified requesters may obtain copies of this report from DBC."
- (2) "Foreign announcement and dissemination of this report by DDC is not authorized."
- (3) "U. S. Government agencies may obtain copies of this report directly from DDC. Other qualified DDC users shall request through _____."
- (4) "U. S. military agencies may obtain copies of this report directly from DDC. Other qualified users shall request through _____."
- (5) "All distribution of this report is controlled. Qualified DDC users shall request through _____."

If the report has been furnished to the Office of Technical Services, Department of Commerce, for sale to the public, indicate this fact and enter the price, if known.

11. SUPPLEMENTARY NOTES: Use for additional explanatory notes.

12. **SPONSORING MILITARY ACTIVITY:** Enter the name of the departmental project office or laboratory sponsoring (paying for) the research and development. Include address.

13. **ABSTRACT:** Enter an abstract giving a brief and factual summary of the document indicative of the report, even though it may also appear elsewhere in the body of the technical report. If additional space is required, a continuation sheet shall be attached.

It is highly desirable that the abstract of classified reports be unclassified. Each paragraph of the abstract shall end with an indication of the military security classification of the information in the paragraph, represented as (TS), (S), (C), or (U).

There is no limitation on the length of the abstract. However, the suggested length is from 150 to 225 words.

14. KEY WORDS: Key words are technically meaningful terms or short phrases that characterize a report and may be used as index entries for cataloging the report. Key words must be selected so that no security classification is required. Identifiers, such as equipment model designation, trade name, military project code name, geographic location, may be used as key words but will be followed by an indication of technical context. The assignment of links, rules, and weights is optional.